

# Distant multipartite entanglement in a first order phase transition

J. Stasińska,<sup>1,2</sup> B. Rogers,<sup>3</sup> M. Paternostro,<sup>3</sup> G. De Chiara,<sup>3</sup> and A. Sanpera<sup>4,1</sup>

<sup>1</sup>*Departament de Física. Universitat Autònoma de Barcelona, E08193 Bellaterra, Spain*

<sup>2</sup>*ICFO-Institut de Ciències Fotòniques. E08860 Castelldefels, Spain*

<sup>3</sup>*Centre for Theoretical Atomic, Molecular and Optical Physics,  
Queen University Belfast, Belfast BT7 1NN, United Kingdom*

<sup>4</sup>*ICREA-Institució Catalana de Recerca i Estudis Avançats, E08011 Barcelona*

We exploit rotationally invariant states as a reference test bed to detect beyond nearest-neighbor genuine tripartite entanglement in spin-1/2 models. We construct multipartite entanglement witnesses which act on a rotationally invariant subspace and use them to detect multipartite entanglement also in non rotationally invariant states. We exemplify our findings by analyzing in detail the anisotropic XXZ spin chain close to its phase transitions. We show how the emergence of multipartite entanglement between non-adjacent spins signals the breaking of the global  $SU(2)$  symmetry, a feature that is not captured by bipartite entanglement.

PACS numbers: 03.65.Ud, 75.10.Pq, 03.67.Mn

The characterization of quantum correlations is a crucial tool for understanding the structure of many-body systems. So far, their study has been mostly based on their linear response to an external perturbation, the behavior of order parameters or low order correlation functions. Recently, the study of the entanglement content of strongly correlated many-body systems have provided new useful insights [1].

The role of entanglement becomes particularly manifest in the study of quantum phase transitions (QPT), closely linked to quantum correlations. Nearest-neighbor and next-nearest neighbor pairwise entanglement, as measured e.g. by the concurrence, unambiguously points out the critical point in the 1D quantum Ising model [2, 3] while for distant spins pairwise entanglement becomes strictly zero. An interesting way to analyze the spatial extension of entanglement is provided by the concept of localizable entanglement introduced in Ref. [4]. For a given multiparty state,  $\rho_{1,2,\dots,N}$  of  $N$  parties, the localizable entanglement is the maximum average entanglement that can be made sharable between two pre-determined parties (say, 1 and 2), by performing general local measurements on the rest of the parties. In Ref. [4] Verstraete *et al.* give examples of QPTs with the property that the correlation length is finite in the vicinity of the critical points, however the (localizable) entanglement length diverges.

While these examples concern bipartite entanglement, the genuine multipartite scenario is much less explored, even though it is believed to play an important role in many-body systems. The presence of genuine multipartite entanglement (GME) was shown in ground states of certain spin models [5–8] and its presence in QPT has been long discussed (see e.g. [10] and references therein).

Here we demonstrate that GME can reveal properties of the many-body systems that are undetectable by bipartite entanglement. This is the case of the transition towards the ferromagnetic phase in the XXZ spin-1/2

chain. In fact, near this critical point, bipartite entanglement properties become independent of the distance between subsystems [11, 12]. In contrast, we find that multipartite entanglement between distant sites depends strongly on the choice of spins thus signalling ground state properties not captured by bipartite entanglement.

Our GME analysis stems from rotationally invariant states of three qubits, whose entanglement properties have been unambiguously characterized by Eggeling and Werner [13] with a set of scalar inequalities. Notice that by projecting a generic state on the rotationally invariant subspace, we can also address GME in non rotationally invariant states. Equivalently, one can detect the GME by constructing appropriate rotationally invariant entanglement witnesses.

Before proceeding further, we briefly review the characterization of rotationally invariant states, provide a geometrical description of such space for real states and construct a family of entanglement witnesses tangent to the set of rotationally invariant biseparable states. We then analyze in detail the entanglement properties of the XXZ model and show the emergence of distant multipartite entanglement in the vicinity of the transition towards the ferromagnetic phase.

The class of  $SO(3)$  invariant states  $\rho$  is defined as:

$$\left\{ \rho : \forall_{\hat{n}, \theta} \left[ \mathcal{D}_{\hat{n}, \theta}^{j_1} \otimes \mathcal{D}_{\hat{n}, \theta}^{j_2} \otimes \mathcal{D}_{\hat{n}, \theta}^{j_3}, \rho \right] = 0 \right\}, \quad (1)$$

where  $\mathcal{D}_{\hat{n}, \theta}^{j_i}$  denotes the unitary irreducible representation of the rotations  $R(\hat{n}, \theta)$  from the  $SO(3)$  group.

For three qubits,  $\rho$  acts trivially in the two subspaces of total angular momentum 1/2 and the one of 3/2. However, since in general  $[\rho, \mathbf{J}_{12}] \neq 0$  with  $\mathbf{J}_{12} = \mathbf{j}_1 + \mathbf{j}_2$  the two subspaces with total  $J = 1/2$  can be mixed. Denoting by  $P_{1/2, a(b)}(\theta, \phi)$  the two orthogonal projectors onto the mixed  $J = 1/2$  subspaces, parametrized by the angles  $\theta$  and  $\phi$ , and by  $P_{3/2}$  the projector onto the subspace

$J = 3/2$ , the density operator can be expressed as

$$\rho = \frac{p}{2}P_{1/2,a}(\theta, \phi) + \frac{q}{2}P_{1/2,b}(\theta, \phi) + \frac{1-p-q}{4}P_{3/2}, \quad (2)$$

where  $0 \leq p, q \leq 1$ . Hence 4 real parameters  $p, q, \theta, \phi$  describe the set of 3-qubit  $SO(3)$ -invariant states. The construction can be extended to higher spins, however, the number of parameters grows dramatically. For instance, for spin-1 particles 13 variables are required. Since the groups  $SO(3)$  and  $SU(2)$  are isomorphic, the above representation can be straightforwardly mapped onto the one for  $SU(2)$  invariant states [13]:

$$\rho = \sum_{k=+,0,1,2,3} \frac{r_k}{4} R_k, \quad (3)$$

where  $r_k = \text{tr} \rho R_k$  and the factor  $1/4$  ensures the normalization. The Hermitian operators  $R_k$  are:  $R_+ = 1/6(1 + V_{12} + V_{23} + V_{13} + V_{123} + V_{321})$ ,  $R_0 = 1/3(21 - V_{123} - V_{321})$ ,  $R_1 = 1/3(2V_{23} - V_{13} - V_{12})$ ,  $R_2 = 1/\sqrt{3}(V_{12} - V_{13})$ ,  $R_3 = i/\sqrt{3}(V_{123} - V_{321})$ , where  $V_{ij}$  is the permutation or swap operator acting on qubits  $i$  and  $j$ ;  $V_{123} = V_{12}V_{23}$  and  $V_{321} = V_{23}V_{12}$  are the two operators which cyclically permute all three particles and  $1$  denotes the identity.

The operator  $R_+$  is proportional to the projector  $P_{3/2}$  and the operator  $R_0$  to  $P_{1/2} = P_{1/2,a} + P_{1/2,b}$ . The three remaining matrices  $R_i$  ( $i = 1, 2, 3$ ) act on the 4-dimensional subspace of total spin  $1/2$ , follow the angular momentum commutation rules and are therefore traceless. In order to ensure that Eq. (3) represents a state, the coefficients  $r_k$  must satisfy:  $r_+, r_0 \geq 0$ ;  $r_+ + r_0 = 1$ , and  $r_1^2 + r_2^2 + r_3^2 \leq r_0^2$ .

The entanglement characterization of three-qubit states distinguishes four classes [14–16]: (i) separable states  $\mathcal{S}$  of the form  $\rho = \sum_i \lambda_i \rho_i^{(1)} \otimes \rho_i^{(2)} \otimes \rho_i^{(3)}$ , (ii) biseparable states  $\mathcal{B}$  belong to the convex hull of states separable with respect to one of the partitions  $1|23$ ,  $2|13$  or  $3|12$  denoted by  $\mathcal{B}_1$ ,  $\mathcal{B}_2$ ,  $\mathcal{B}_3$ , respectively, and two GME classes (iii) W-type states, and (iv) GHZ-type states. Each class embraces those that are lower in the hierarchy,  $\mathcal{S} \subset \mathcal{B} \subset \mathcal{W} \subset \text{GHZ}$ . The distinction between the W-type states and the GHZ-type states arises from the fact that for three qubits there exist two stochastic local operations and classical communications inequivalent classes of genuinely entangled states with representative elements being precisely the W state  $|W\rangle = 1/\sqrt{3}(|100\rangle + |010\rangle + |001\rangle)$ , and the GHZ state  $|\text{GHZ}\rangle = 1/\sqrt{2}(|000\rangle + |111\rangle)$ . Therefore, the W and GHZ classes are formed by convex combinations of states equivalent to  $|W\rangle$  and of combinations of states equivalent to  $|\text{GHZ}\rangle$ .

In Ref. [13], the subsets  $\mathcal{S}$  and  $\mathcal{B}$  of the  $SU(2)$  invariant states are fully described in terms of inequalities for the coefficients  $r_k$ . In particular, the set  $\mathcal{S}$  is constrained by the following conditions:  $1/4 \leq r_+ \leq 1$ ;  $3r_3^2 + (1 -$

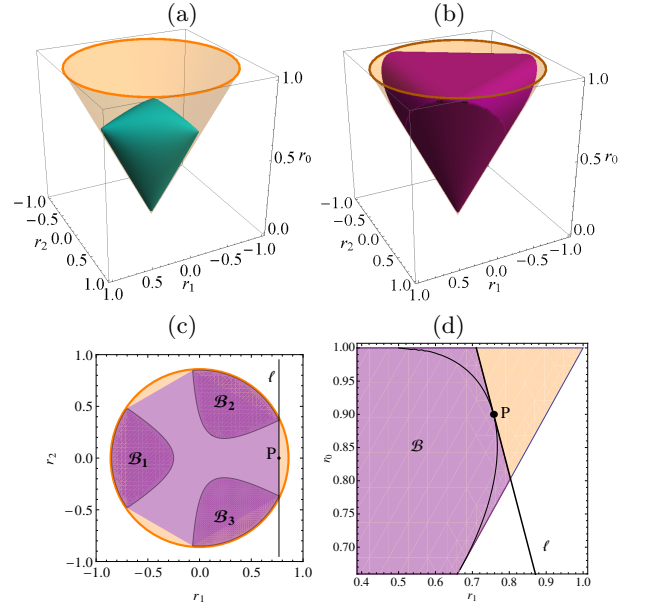


FIG. 1: (Color online) Graphical representation of the set of real rotationally invariant states and its subsets with various types of entanglement in the space of  $r_0, r_1, r_2$ . (a) Separable and (b) biseparable states. (c) A horizontal cut showing the three set of biseparable states, their convex hull and the tangent in the point  $P$  to the set representing the optimal witness. (d) Same as in (c) but a vertical is shown.

$3r_+)^2 \leq (r_1 + r_+)[(r_1 - 2r_+)^2 - 3r_2^2]$ . Analogously, the states belonging to the set  $\mathcal{B}_1$ , can be shown to fulfill the condition  $3(r_2^2 + r_3^2) \leq (1 - |m|)^2 - [(r_1 - r_+) - |m|]^2$  and  $|m| < 1$  where  $m = 1 + r_1 - 2r_+$ . The corresponding sets  $\mathcal{B}_2$  and  $\mathcal{B}_3$  are found by rotating  $\mathcal{B}_1$  by  $\pm 2\pi/3$  around the axis  $r_0$ . Finally, the set  $\mathcal{T}$  of genuine tripartite entangled states is found as the complement of  $\mathcal{B}$  in the set of all states. Interestingly, it was shown that for some of those genuine tripartite entangled states a local hidden-variable model exists [17] similarly to the case of the bipartite Werner states [18]. Similar classes have been recently investigated in the context of symmetric GHZ states [19].

For real Hamiltonians, a very common situation in spin systems, the above description is further simplified as their ground states and their reductions are represented by real density operators. This is equivalent to setting  $\phi = 0$  in (2) or  $r_3 = 0$  in (3) and allows us to visualize the set of rotationally invariant states in the space  $r_1, r_2, r_0$  (Fig. 1). The complete set is a cone with symmetry axis parallel to the axis  $r_0$ . In Fig. 1(a-b) we depict the set of separable  $\mathcal{S}$  and biseparable  $\mathcal{B}$  states, respectively; the complementary volume contains genuine tripartite entangled states. Fig. 1(c) show a horizontal section of the cone for a fixed  $r_0$  and Fig. 1(d) a vertical section. We notice that a necessary condition for a state to be tripartite entangled is  $r_0 > 2/3$ . In fact below this value

biseparable states fill the cone completely.

The above criteria can be extended to all states using the *twirling map* that projects each state onto its rotational invariant subspace:  $\Pi\rho = \int_G d\mathcal{U} \mathcal{U}\rho \mathcal{U}^\dagger$  where  $G$  consists of local unitaries  $\mathcal{U} = U \otimes U \otimes U$ . The following statements now hold: (i)  $\Pi\rho$  is  $SU(2)$  invariant (ii) if  $\rho$  is separable then  $\Pi\rho$  is separable [20], (iii) if  $\Pi\rho$  is biseparable then  $\rho$  is not separable and (iv) if  $\Pi\rho$  is genuine tripartite entangled so is  $\rho$ .

The geometrical description of the Hilbert space depicted in Fig. 1 facilitates the construction of a multipartite entanglement witness, i.e. an observable  $W$ , such that,  $\forall \rho \in \mathcal{B}$ ,  $\text{tr} W\rho \geq 0$  and there exists at least one state  $\rho \in \mathcal{T}$ :  $\text{tr} W\rho < 0$ . It suffices to choose a witness of the form  $W = \sum_i c_i R_i$ , where  $i \in \{+, 0, 1, 2\}$ , so its expectation value with a rotationally invariant state simplifies to a scalar product  $\text{tr}(W\rho) = \sum_i c_i r_i \equiv \mathbf{c} \cdot \mathbf{r}$ . We determine  $\mathbf{c}$  using the geometric description of the witness as a plane intersecting the cone of rotationally invariant states and tangent to the set  $\mathcal{B}$  in the point  $\mathbf{P}$  with normal vector  $\hat{\mathbf{u}}$  (see Fig. 1(d)). We find  $\text{tr}(W\rho) = \hat{\mathbf{u}} \cdot (\mathbf{r} - \mathbf{P})$ , and from the definition of  $\mathbf{c}$  we obtain  $W = u_0 R_0 + u_1 R_1 + u_2 R_2 - \hat{\mathbf{u}} \cdot \mathbf{P}$ . The witness plane is calculated with  $\mathbf{P}$  in the midpoint of the line between the biseparable subsets  $\mathcal{B}_2$  and  $\mathcal{B}_3$ . It also clearly depends on the choice of  $r_0$ :

$$W(r_0) = \left(1 + \frac{\sqrt{3}}{2} \frac{2 - 3r_0}{\sqrt{-1 + 4r_0 - 3r_0^2}}\right) R_0 - R_1 - \left(\frac{\sqrt{3}(1 - 2r_0)}{2\sqrt{-1 + 4r_0 - 3r_0^2}} + \frac{1}{2}\right) \mathbf{1}. \quad (4)$$

The witness can then be rotated about the  $r_0$  axis by  $\pm 2\pi/3$  to obtain witnesses planes tangential to  $\mathcal{B}$  on the lines between  $\mathcal{B}_1$  and  $\mathcal{B}_2$ , or  $\mathcal{B}_1$  and  $\mathcal{B}_3$ , respectively. The explicit derivation of Eq. (4) and the demonstration that  $W$  is indeed a witness can be found in the Appendix.

With all these tools in hand, we can now analyze the entanglement structure of spin chain models beyond the bipartite case. To this aim we study genuine multipartite entanglement in an open chain of size  $N$  subject to the XXZ Hamiltonian

$$H_{\text{XXZ}} = \sum_{i=1}^{N-1} [J(\sigma_i^x \sigma_{i+1}^x + \sigma_i^y \sigma_{i+1}^y) + \lambda \sigma_i^z \sigma_{i+1}^z], \quad (5)$$

where  $\lambda$  is the anisotropic parameter. For lattices with even  $N$  (and also in the thermodynamic limit) the sign of  $J$  is irrelevant since it is possible to change  $\sigma_i^x \rightarrow -\sigma_i^x$  and  $\sigma_i^y \rightarrow -\sigma_i^y$  for all even (odd) sites, thus the Hamiltonian is  $SU(2)$  invariant for  $\lambda/J = \pm 1$ . For any value of  $\lambda$ ,  $H_{\text{XXZ}}$  is  $U(1)$  invariant. For non bipartite lattices (or odd  $N$ ) geometrical frustration can appear. In what follows, we assume without loss of generality that  $J = 1$ .

The complete phase diagram of the model is well known: the ground state is ferromagnetic for  $\lambda \leq -1$ ,

XY-critical for  $-1 < \lambda < 1$ , and Ising-antiferromagnetic (Néel) otherwise. At  $\lambda = -1$  a first order transition separates the ferromagnetic and critical phases. This point is not conformal and has recently attracted some attention [11, 12]. Here we focus on the multipartite entanglement content in the vicinity of this phase transition. Before proceeding further, notice that at  $\lambda = -1$  the highly degenerate ground state is in the  $SU(2)$  isotropic ferromagnetic multiplet spanned by any state with maximum total angular momentum  $J$ :  $|J = N/2, J_z\rangle$  for all possible values of  $J_z$ . Neither of these states exhibit finite size corrections to the energy per site, nor are they rotational invariant. However, each of them corresponds to a symmetric Dicke state, i.e.,  $|J = N/2, J_z = (2k - N)/2\rangle = 1/\sqrt{C_k^N} \sum |\mathcal{P}(1^{(k)}, 0^{(N-k)})\rangle$ , with  $k$  subsystems in the state  $|1\rangle$  and the remaining in the state  $|0\rangle$ ;  $\mathcal{P}$  are the elements of the permutation group,  $C_k^N$  is the binomial coefficient, and  $\{|1\rangle, |0\rangle\}$  is the computational basis (spin up, spin down). Thus, the interchange between any two spins leaves the corresponding Dicke state unchanged and by construction any linear combination as well. In the region  $-1 < \lambda < 1$ , the total spin,  $J$ , is not well defined but  $J_z = 0$ . In the limit  $\lambda \rightarrow -1^+$  the ground state was found numerically to be an equally weighted superposition of all the elements of the standard basis within the sector  $J_z = 0$  [12]. Finally, notice that for  $\lambda = +1$ , the ground state is a rotationally invariant singlet with  $J = 0$ .

We analyze now the entanglement content of the model by computing both the bipartite concurrence  $C_N(\rho_{i,i+r})$  of two qubits at distance  $r$  as well as the mean value of the entanglement witness (4),  $\text{tr}(W\rho_{i,j,k})$ , for three qubits  $i, j, k$ . Concurrences can be analytically obtained in the  $SU(2)$  multiplet after realizing that any reduction of a multipartite symmetric Dicke state  $|N/2, k\rangle$  is also symmetric, i.e. independent of  $r$  and  $i$ , and read [21]:

$$C_N(\rho_{i,i+r}) = 2\max(0, \rho_{01,01} - \sqrt{\rho_{00,00}\rho_{11,11}}) \quad (6) \\ = \frac{(N^2 - 4J_z^2) - \sqrt{(N^2 - 4J_z^2)[(N - 2)^2 - 4J_z^2]}}{2N(N - 1)}$$

since the only non-zero matrix elements  $\rho_{i,i+r}$  are the symmetric ones given by  $\rho_{00,00}(\rho_{11,11}) = (N \pm 2k)(N - 2 \pm 2k)/(4N(N - 1))$ ,  $\rho_{01,01}(01,10)(10,01)(10,10) = (N^2 - 4k^2)/(4N(N - 1))$ . As previously noted, the value of the concurrence for large  $N$  is very small and close to the exact value  $C_N = 1/(N - 1)$  achieved for  $J_z = 0$  ( $k = N/2$ ). Thus, for large  $N$ , all members of the  $SU(2)$  multiplet (except the trivially separable  $|N/2, \pm N/2\rangle$ ) have equal concurrences which tend to zero in the thermodynamic limit.

Let us now discuss our results. We compute the ground state of  $H_{\text{XXZ}}$  for the whole phase diagram using the density matrix renormalization group (DMRG) [22] for open chains of up to 192 sites. From the ground state, we construct the reduced density matrix of either two or three

spins (not necessarily adjacent) close to the centre of the chain and calculate the corresponding concurrences as well as the tripartite entanglement by means of the entanglement witness (4) for the whole phase diagram. There exist suitable multipartite entanglement witnesses that detect GME of adjacent sites for two-body models [8, 9] or global GME of Dicke states based on two-point correlation functions [23]. Our method, however, allows us to choose our reduced system at will without imposing further symmetries.

Our results are summarized in Fig. 2(a), where we display  $C(\rho_{i,i+r})$  for different values of  $r$  as a function of  $\lambda$ , and in particular near the isotropic point  $\lambda = -1$ . The concurrences for the complete phase diagram are reported in the Appendix. In accordance with previous results based on bipartite measures [12], we observe that close to the isotropic ferromagnetic point (i.e.  $\lambda = -0.999$ ) all concurrences for  $N \gg 1$  collapse to the same value  $1/(N-1)$ . Also, the study of the entanglement spectrum shows such symmetry in the limit  $\lambda \rightarrow -1^+$  [11].

To investigate whether or not this feature of bipartite entanglement is shared also by the multipartite structure we investigated the minimum mean value of the witness  $\text{tr}(W\rho_{i,i+r,i+r'})$  for different spin arrangements (the spin  $i$  is near the middle of the chain to avoid finite-size effects). For adjacent sites  $(i, i+1, i+2)$  we recover previous results [8] indicating the presence of GME for  $\lambda > -1$ . However, for non adjacent spins GME appears only for  $\lambda \rightarrow -1^+$  and, contrary to the concurrence, depends strongly on the chosen spins and on their relative distances. For instance, we find that long-range GME exists for the arrangement  $(i, i+1, i+r)$ ,  $r > 1$  as shown in Fig. 2(b). Long-range GME exists also for other spin-arrangements  $i, j, k$  when at least two sites indexes have different parity (see the Appendix). Our results provide evidence that (i) distant multipartite entanglement is present in the system; (ii) contrary to previous results, based on the concurrence, the global  $SU(2)$  symmetry is already broken very close to the QPT, evidencing the sensitivity of  $W$  to the fine ground state structure.

As we demonstrated for the ground state of the XXZ model, the method we provide is not restricted to  $SU(2)$  invariant states and can be applied to any 3-qubit states. It can also be extended to ground and thermal states of spin-1/2 Hamiltonians in any lattice geometry, not only 1D. Notice however that while the detection of GME for  $SU(2)$  invariant states is unambiguous, the negativity of the expectation value of the witness  $\langle W \rangle$  is in general only a sufficient condition for GME.

Summarizing, in this work we have provided a deeper insight in the quantum correlations structure of the many-body ground state of a spin chain close to a first order quantum phase transition, beyond the standard framework of bipartite entanglement. We have shown that an intricate multipartite entanglement structure

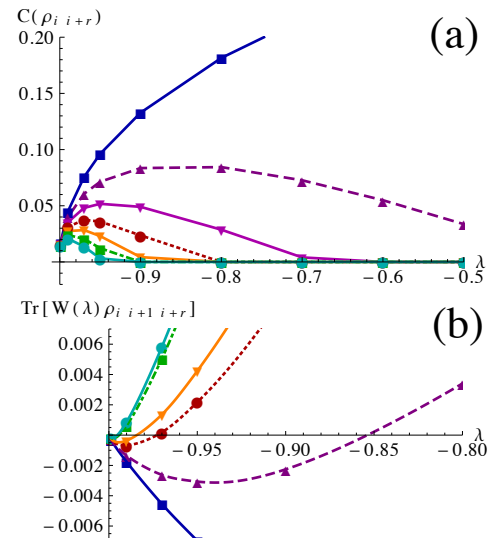


FIG. 2: (color online) (a) Concurrences of a reduced state of two non-adjacent spins  $\rho_{i,i+r}$  ( $r = 1, \dots, 7$  from top to bottom); (b) Mean value of the rotationally-invariant entanglement witness detecting genuine tripartite entanglement for reduced states of three non-adjacent spins  $\rho_{i,i+1,i+r}$ . GME emerges in each case as  $\lambda \rightarrow -1^+$  ( $r = 2, \dots, 7$  from the bottom to the top). The reduced density matrices have been calculated using DMRG simulations with  $N=96$ .

emerges when approaching the critical point. GME allows us to study the breaking of the global  $SU(2)$  and permutational symmetries underpinning the phase transition.

We thank R. Augusiak, J. Calsamiglia, A. Läuchli, R. Muñoz-Tapia, and J. Serra for useful discussions. We acknowledge financial support from the Spanish MINECO (FIS2008-01236), European Regional development Fund, Generalitat de Catalunya Grant No. SGR2009-00347. MP acknowledges the UK EPSRC for a Career Acceleration Fellowship and a grant from the "New Directions for EPSRC Research Leaders" initiative (Grant No. EP/G004759/1).

- 
- [1] L. Amico, R. Fazio, A. Osterloh, and V. Vedral, *Rev. Mod. Phys.* **80**, 517 (2008).
  - [2] T. Osborne and M. Nielsen, *Phys. Rev. A* **66**, 032110 (2002).
  - [3] A. Osterloh, L. Amico, G. Falci, and R. Fazio, *Nature* **416**, 608 (2002).
  - [4] F. Verstraete, M. Popp, and J. I. Cirac, *Phys. Rev. Lett.* **92**, 027901 (2004).
  - [5] X. Wang, *Phys. Rev. A* **66**, 044305 (2002).
  - [6] P. Štelmachovič and V. Bužek, *Phys. Rev. A* **70**, 032313 (2004).
  - [7] D. Bruß, N. Datta, A. Ekert, L. Kwak, and C. Macchiavello, *Phys. Rev. A* **72**, 014301 (2005).
  - [8] O. Gühne, G. Toth, and H. J. Briegel, *New J. Phys.* **7**,

- 229 (2005).
- [9] O. Gühne and G. Toth, Phys. Rev. A **73**, 052319 (2006).
  - [10] T. de Oliveira, G. Rigolin, M. de Oliveira, and E. Miranda, Phys. Rev. Lett. **97**, 170401 (2006).
  - [11] V. Alba, M. Haque, and A. M. Läuchli, J. Stat. Mech. P08011 (2012).
  - [12] L. Banchi, F. Colomo, and P. Verrucchi, Phys. Rev. A **80**, 022341 (2009).
  - [13] T. Eggeling and R. F. Werner, Phys. Rev. A **63**, 042111 (2001).
  - [14] W. Dür and J. I. Cirac, Phys. Rev. A **61**, 042314 (2000).
  - [15] A. Acín, D. Bruß, M. Lewenstein, and A. Sanpera, Phys. Rev. Lett. **87**, 040401 (2001).
  - [16] M. Huber and J. I. de Vicente, Phys. Rev. Lett. **110**, 030501 (2013).
  - [17] G. Tóth and A. Acín, Phys. Rev. A **74**, 030306(R) (2006).
  - [18] R. F. Werner, Phys. Rev. A **40**, 4277 (1989).
  - [19] C. Eltschka and J. Siewert, Phys. Rev. Lett. **108**, 020502 (2012).
  - [20] K. Vollbrecht and R. F. Werner, Phys. Rev. A **64**, 062307 (2001).
  - [21] X. Wang and K. Mølmer, Eur. Phys. J. D **18**, 385 (2002).
  - [22] S. R. White, Phys. Rev. Lett. **69**, 2863 (1992); G. De Chiara et al., J. Comp. Theor. Nanos. **5**, 1277 (2008).
  - [23] P. Krammer, H. Kampermann, D. Bruß, R. A. Bertlmann, L. C. Kwek, and C. Macchiavello, Phys. Rev. Lett. **103**, 100502 (2009).

## Appendix A: Construction of the witness operator

A plane tangent to the surface of the set of biseparable states is uniquely characterised by a point  $\mathbf{P}$  and a normal unit vector  $\hat{\mathbf{u}}$ . We choose the point lying on the line between sets  $\mathcal{B}_2$  and  $\mathcal{B}_3$  (later denoted by  $\ell$ ) and define a curve parametrized by  $r_0$  as

$$\mathbf{P}(r_0) = \left[ r_0, \frac{-1 + 2r_0 + \sqrt{3}\sqrt{-1 + 4r_0 - 3r_0^2}}{2}, 0 \right] \quad (7)$$

with  $r_0 > 2/3$ . Then the normal vector  $\hat{\mathbf{u}}$  is the cross-product of the vector tangent to the curve  $\mathbf{P}(r_0)$ :

$$\mathbf{v}_1 = \frac{d}{dr_0} \mathbf{P}(r_0) = \left[ 1, 1 + \frac{\sqrt{3}}{2} \frac{2 - 3r_0}{\sqrt{-1 + 4r_0 - 3r_0^2}}, 0 \right], \quad (8)$$

and the vector  $\mathbf{v}_2 = (0, 0, 1)$  parallel to the  $\ell$ . Therefore, we have

$$\begin{aligned} \hat{\mathbf{u}} &= \frac{\mathbf{v}_1 \times \mathbf{v}_2}{\|\mathbf{v}_1\|} \\ &= \frac{1}{\|\mathbf{v}_1\|} \left[ 1 + \frac{\sqrt{3}}{2} \frac{2 - 3r_0}{\sqrt{-1 + 4r_0 - 3r_0^2}}, -1, 0 \right]. \end{aligned} \quad (9)$$

Substituting Eq. (9) in the expression of the witness:

$$W = u_0 R_0 + u_1 R_1 + u_2 R_2 - \hat{\mathbf{u}} \cdot \mathbf{P}, \quad (10)$$

we obtain the unnormalized witness in the following form

$$\begin{aligned} W(r_0) &= \left( 1 + \frac{\sqrt{3}}{2} \frac{2 - 3r_0}{\sqrt{-1 + 4r_0 - 3r_0^2}} \right) R_0 \\ &\quad - R_1 - \left( \frac{\sqrt{3}(1 - 2r_0)}{2\sqrt{-1 + 4r_0 - 3r_0^2}} + \frac{1}{2} \right) \mathbf{1}. \end{aligned} \quad (11)$$

The other two witnesses obtained by rotation of the witness plane by  $\pm 2\pi/3$  are

$$\begin{aligned} W(r_0) &= \left( 1 + \frac{\sqrt{3}}{2} \frac{2 - 3r_0}{\sqrt{-1 + 4r_0 - 3r_0^2}} \right) R_0 \\ &\quad - \left( \frac{1}{2} R_1 \pm \frac{\sqrt{3}}{2} R_2 \right) \\ &\quad - \left( \frac{\sqrt{3}(1 - 2r_0)}{2\sqrt{-1 + 4r_0 - 3r_0^2}} + \frac{1}{2} \right) \mathbf{1}. \end{aligned}$$

By construction the operator  $W$  is positive for all biseparable rotationally invariant states, even those with an imaginary component since  $\text{tr}(WR_3) = 0$ . Furthermore,  $W$  is an entanglement witness for genuine tripartite entangled states, i.e., it is positive for all biseparable states. For this purpose it is enough to show that  $\langle ef | W | ef \rangle \geq 0$  for all  $|ef\rangle$  being product vectors with respect to bipartitions  $12|3$ ,  $1|23$ ,  $13|2$ . Without loss of generality we focus on the specific partition and have:

$$\begin{aligned} \langle e_{12}f_3 | W | e_{12}f_3 \rangle &= \langle e_{12}f_3 | \int d\mathbf{U} \mathbf{U}^\dagger W \mathbf{U} | e_{12}f_3 \rangle \\ &= \text{tr}(\Pi | e_{12}f_3 \rangle \langle e_{12}f_3 | W) \geq 0 \end{aligned} \quad (12)$$

where we use the fact that  $W$  is rotationally invariant and that the state  $\Pi | e_{12}f_3 \rangle \langle e_{12}f_3 |$  is rotationally invariant and either biseparable or separable. Note that Eq. (12) establishes equivalence between the biseparability test based on the witness and the twirling criterion for all real density matrices.

## Appendix B: Further results on concurrence and GME

We computed the ground state of  $H_{\text{XXZ}}$  for the whole phase diagram using the density matrix renormalization group (DMRG) [22] for open chains up to 192 sites. From the ground state, we construct the reduced density matrix either of two or three spins (not necessarily adjacent) close to the centre of the chain and check the presence of bipartite entanglement (by means of concurrence) and the tripartite entanglement (by means of the entanglement witness) for the whole phase diagram. In Fig. 3 we display the concurrence,  $C(\rho_{i,i+r})$ , for spins at distance  $r$  as a function of  $\lambda$ , and in particular near the isotropic point  $\lambda = -1$  (inset).

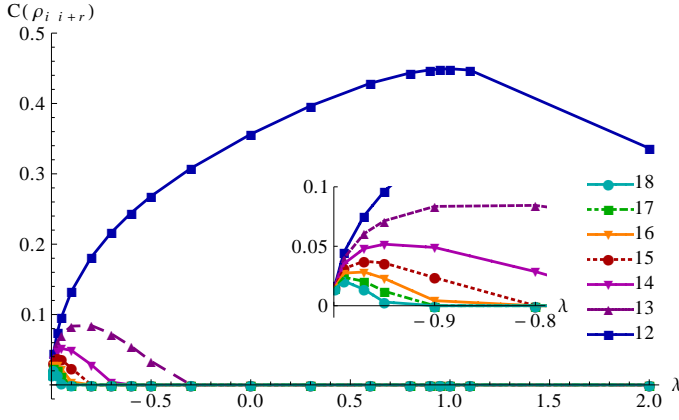


FIG. 3: (Color online) Concurrences of a reduced state of two non-adjacent spins  $(i, i+r)$ . For  $N \gg 1$  all the concurrences collapse to the same value:  $1/(N-1)$  close to the isotropic ferromagnetic point  $\lambda = -1^+$ . The reduced density matrices have been calculated using DMRG simulations with  $N=96$ . For convenience the spin arrangements are denoted as 12, 13, ..., however the entanglement is studied close to the middle of the chain.

In Fig. 4 we plot the mean value of the entanglement witness introduced in Appendix A for each spin arrangement  $(i, i+r, i+s)$ . The mean value is minimized over the whole family of witnesses. We find that long range GME exists for the arrangement  $(i, i+1, i+2)$  for arbitrary  $\lambda > -1$ , however for the arrangements  $(i, i+1, i+r)$ ,  $r > 2$  GME is present only in the vicinity of the point  $\lambda = -1$ . Long range GME exists also for other spin-arrangements  $i, j, k$  when at least two sites indexes are of different parity. In particular the arrangements  $(i, i+2, i+4)$  and  $(i, i+2, i+6)$  are always separable as shown in the inset of Fig. 4(b)

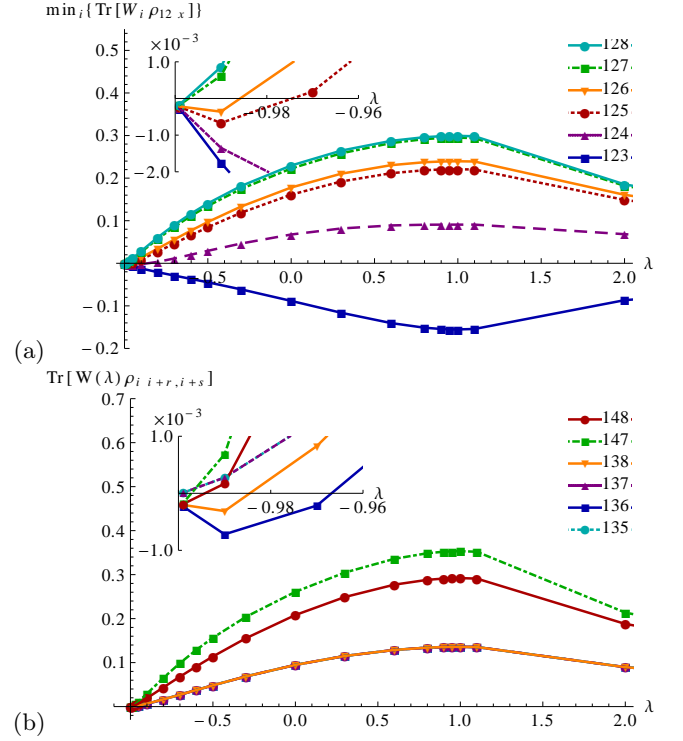


FIG. 4: (Color online) Mean value of the rotationally-invariant entanglement witness detecting genuine tripartite entanglement for reduced states of three non-adjacent spins (a)  $(i, i+1, i+r)$  (b)  $(i, i+r, i+s)$ . As  $\lambda \rightarrow -1^+$  (see the insets) GME emerges in all the arrangements depicted in (a), and those shown in (b) except for (135), (137). The reduced density matrices have been calculated using DMRG simulations with  $N=96$ . For convenience the spin arrangements are denoted as 123, 135, ..., however the entanglement is studied close to the middle of the chain.